Front. Optoelectron. China 2008, 1(1–2): 58–63
DOI 10.1007/s12200-008-0016-2

RESEARCH ARTICLE

Tunable wavelength converters of picosecond pulses based on periodically poled $LiNbO_3$ waveguides

Jian WANG, Junqiang SUN (✉), Qizhen SUN

Wuhan National Laboratory for Optoelectronics, School of Optoelectronic Science and Engineering, Huazhong University of Science and Technology, Wuhan 430074, China

Abstract A tunable wavelength conversion between picosecond pulses is experimentally demonstrated by using cascaded sum- and difference-frequency generation (cSFG/DFG) in a periodically poled $LiNbO_3$ (PPLN) waveguide. The pulsed signal with 40 GHz repetition rate and 1.57 ps pulse width is adopted. When the input signal and the first control wavelengths are kept at 1554.2 and 1532.5 nm, respectively, the output signal wavelength can be tuned from 1536.0 to 1545.2 nm as the second control wavelength varies from 1550.5 to 1541.0 nm. By varying the first control wavelength to satisfy the quasi-phase matching (QPM) condition for sum-frequency generation (SFG) and simultaneously adjusting the second control wavelength, the tunable output signal wavelength can also be obtained when the input signal wavelength is changed. In the experiment, the amplified spontaneous emission (ASE) noise from the erbium-doped fiber amplifier (EDFA) is effectively suppressed by employing two narrow band tunable filters. Therefore, the wavelength down- and up-conversions are simultaneously observed.

Keywords wavelength converter, periodically poled $LiNbO_3$ (PPLN), cascaded sum- and difference-frequency generation (cSFG/DFG), wavelength down- and up-conversions

1 Introduction

The wavelength converter (WC) is regarded as one of the most crucial components to construct future all-optical networks. In addition to the capability of enabling wavelength reuse, avoiding wavelength channel contentions, reconfiguring wavelength switchable optical networks, and enhancing network capacity, WC also helps enable flexible network management and dynamic network construction [1]. The most recent wavelength conversion techniques include the use of cross-gain modulation (XGM) [2], cross-phase modulation (XPM) [3], cross-absorption modulation (XAM) [4], and four-wave mixing (FWM) [5] in semiconductor optical amplifiers (SOAs) as well as second-order nonlinearities in passive optical waveguides [6–18]. Among these conversion schemes, wavelength conversion based on second-order nonlinearities in periodically poled $LiNbO_3$ (PPLN) waveguides has shown distinct advantages [6–18]. Besides the function of switching the information carried by input signal, PPLN-based wavelength conversion has other promising merits such as ultra-fast response, convenience for tunable operation, negligible spontaneous emission noise, and no intrinsic frequency chirp. Several second-order nonlinearities in quasi-phase matching (QPM) PPLN waveguides have attracted increasing attention in recent years, including direct difference-frequency generation (DFG) [9,10], cascaded second-harmonic generation and difference-frequency generation (cSHG/DFG) [10–13], and cascaded sum- and difference-frequency generation (cSFG/DFG) [14–18]. However, most previous researches suffered due to the great limitation on operating at the continuous-wave (CW) situation [9–16]. Although pulsed signals were employed in some experiments [17,18], amplified spontaneous emission (ASE) noise originating from the erbium-doped fiber amplifier (EDFA) was induced in the experimental systems. A negative influence on the wavelength up-conversion was thus introduced and the optical signal-to-noise ratio of the output signal was degraded. It should be noted that control-wavelength tolerance for DFG (0.15 nm) and cSHG/DFG (0.3 nm) is very small [10], making it practically impossible to realize broadband tunable wavelength conversion based on conventional DFG and cSHG/DFG.

Translated from *Acta Optica Sinica*, 2006, 26(10): 1453–1458 [译自: 光学学报]

E-mail: jqsun@mail.hust.edu.cn

In this paper, tunable wavelength conversion of picosecond pulses is experimentally investigated based on cSFG/DFG in a PPLN waveguide. The pulsed signal with a pulse width of 1.57 ps and a repetition rate of 40 GHz is adopted in the experiment. In particular, ASE noise within the long waveband is effectively suppressed by simultaneously using two narrow band tunable filters in the experimental configurations. As a result, simultaneous wavelength down- and up-conversions are observed in the experiment.

2 Operation principle

Figure 1 illustrates the cSFG/DFG processes inside the PPLN waveguide. At the input port of the PPLN waveguide, the input signal (λ_{in}) and two control waves (λ_{C1},λ_{C2}) are simultaneously launched into the waveguide. The input signal and one of the control waves (λ_{C1}) participate in the SFG process under the QPM condition, and the sum-frequency wave (λ_{SF}) is generated. At the same time, the sum-frequency wave interacts with the other control wave (λ_{C2}) to yield the converted wave called output signal (λ_{out}) by the DFG process. It is noted that the output signal is within the same waveband of the input signal and two control waves. Therefore, five optical waves including the generated sum-frequency wave and the output signal during cSFG/DFG processes are obtained at the waveguide's output port. Note that the wavelength of the output signal satisfies the following relationship according to the law of the energy conservation

$$1/\lambda_{out} = 1/\lambda_{SF} - 1/\lambda_{C2} = 1/\lambda_{in} + 1/\lambda_{C1} - 1/\lambda_{C2}. \quad (1)$$

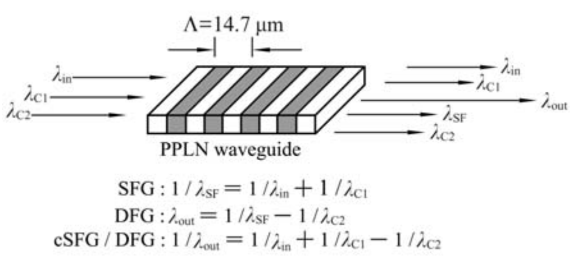

Fig. 1 Schematic diagram of cascaded sum- and difference-frequency generation in a periodically poled $LiNbO_3$ waveguide

It is known that tunable wavelength conversion means that the wavelength of the converted output signal can be tuned flexibly according to the practical requirement for a fixed input signal wavelength. Remarkably, it is difficult to perform such a function using conventional direct DFG and cSHG/DFG processes. However, tunable wavelength conversion can be easily realized by using cSFG/DFG processes. According to Eq. (1), as λ_{in} is fixed, λ_{C1} is properly adjusted to meet the SFG QPM condition, resulting in a fixed sum-frequency wave, and then tunable output of λ_{out} can be conveniently achieved simply by changing λ_{C2}. Obviously, in the cSFG/DFG processes, λ_{C1} is decided by λ_{in} and λ_{C2} depends on λ_{out}.

3 Experimental setup

The experimental setup of the proposed PPLN-based tunable wavelength converter is shown in Fig. 2.

Two control waves provided by two tunable external cavity lasers are combined by a 3 dB coupler and then amplified by a high-power EDFA. Note that at the output port of EDFA, although two control waves are effectively amplified, strong ASE noise is also induced within the gain range of EDFA. To suppress such noise, the output optical waves after EDFA are divided into two paths by another 3 dB coupler, and each path follows a narrow band tunable filter (TF1 and TF2). TF1 and TF2 are used to filter two control waves, respectively. As a result, the ASE noise caused by EDFA will be greatly suppressed. Two amplified control waves with low ASE noise level, together with the pulsed signal generated from a mode-locked fiber ring laser with a pulse width of 1.57 ps and a repetition rate of 40 GHz, are integrated by using a 3×1 coupler. They are then launched into the PPLN waveguide to take part in cSFG/DFG nonlinear interactions after passing through a PC. The obtained converted output signal completely copies the information carried by the input signal, therefore the wavelength conversion from the input signal to the output signal is successfully implemented. The output spectra of the converter are monitored by an optical spectrum analyzer (Anritsu MS9710C) with the highest spectral resolution of 0.05 nm, and temporal waveforms of the input and output signals are observed through a communications signal analyzer (Tektronix CSA 8000B). The EDFA in Fig. 2 has a small-signal gain of 40 dB and a high saturation output power of 30 dBm. The tuning bandwidth and line width of the two tunable filters within the 1.5 μm band are 50 and 1 nm, respectively. The PPLN waveguide has a length of 50 mm, a QPM period of 14.7 μm, a waveguide width of 12 μm, and an initial proton exchange depth of 0.8 μm. It is fabricated by the electric-field poling method and annealing proton-exchanged technique. These parameters allow the QPM wavelength for the SHG process to be about 1543.2 nm at room temperature in the experiment. The fiber-to-fiber coupling loss of the PPLN waveguide, which is estimated at about 4.7 dB, is caused by reflection losses at the uncoated end faces, mode mismatch between the fibers and the PPLN waveguide, and intrinsic waveguide losses.

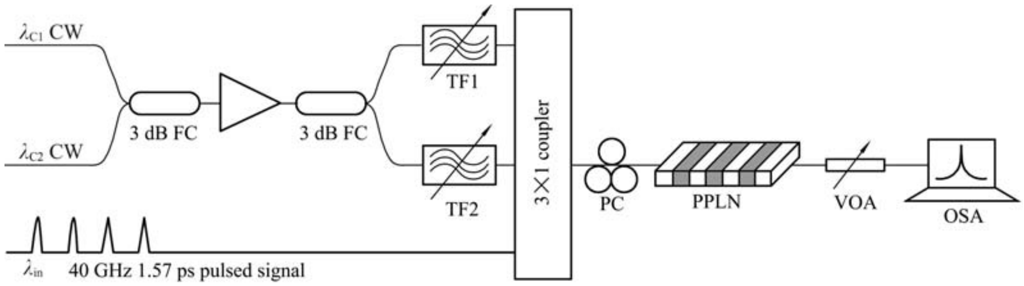

Fig. 2 Experimental setup of PPLN-based tunable wavelength converter. (EDFA: erbium-doped fiber amplifier, FC: fiber coupler, TF: tunable filter, PC: polarization controller, VOA: variable optical attenuator, OSA: optical spectrum analyzer)

4 Experimental results and analyses

Figure 3 shows the measured output spectra from the tunable wavelength converter for different wavelengths of the second control wave. It can be clearly seen from Fig. 3 that tunable wavelength conversion is realized by using cSFG/DFG processes. The center wavelength of the input signal is set at 1554.4 nm, and the wavelength of the first control wave is adjusted at about 1532.5 nm to satisfy the SFG QPM condition. It is found that the wavelength of the output signal can be tuned from 1536.0 to 1545.2 nm as the wavelength of the second control wave is changed from 1550.5 to 1541.0 nm.

Figure 4 depicts the measured output spectra from the tunable wavelength converter for different wavelengths of the second control wave when changing the wavelength of the input signal to 1548.9 nm. In this case the wavelength of the first control wave is correspondingly adjusted at about 1536.7 nm to meet the SFG QPM condition. By changing the wavelength of the second control wave from 1554.5 to 1528.4 nm, the wavelength of the output signal can be tuned from 1531.7 to 1558.4 nm.

Remarkably, as shown in Figs. 3 and 4, ASE noise within the wavelength range of 1525.0 to 1565.0 nm is effectively suppressed due to the use of two tunable filters. It can be seen that the datum line of the optical spectra at both short- and long-wavebands have almost the same height, i.e., ASE noise over the whole wavelength range (1525.0–1565.0 nm) remains at a low

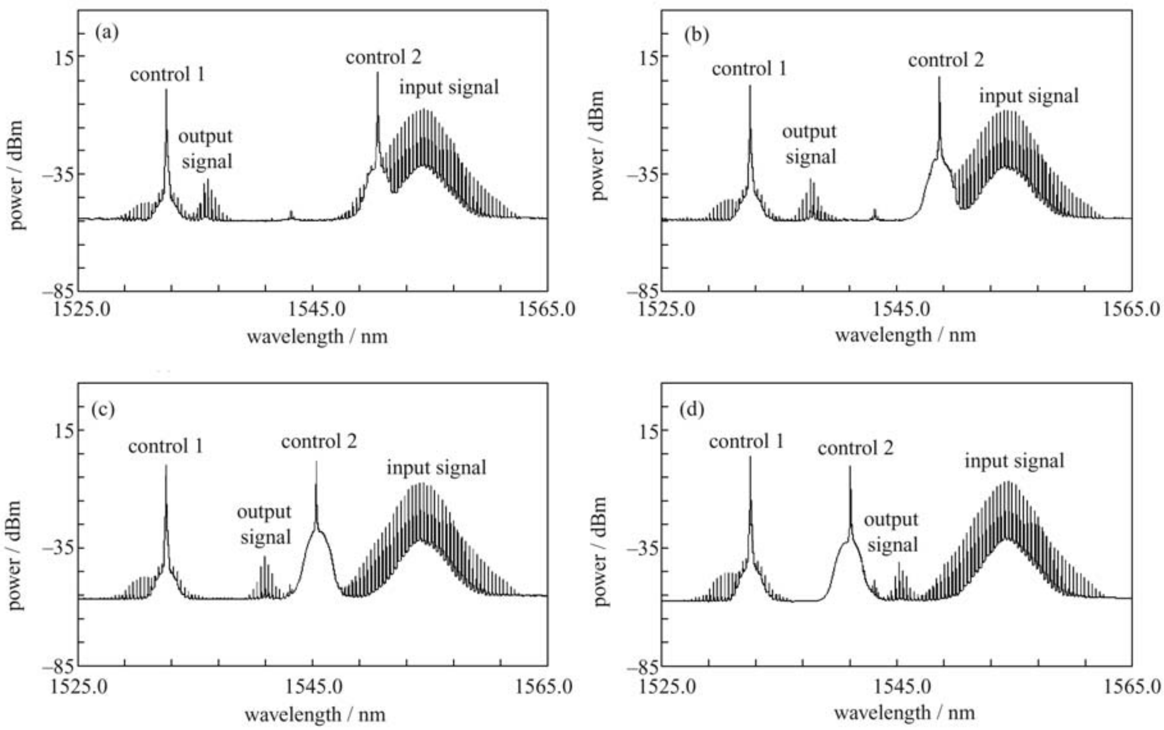

Fig. 3 Measured output spectra from tunable wavelength converter for different wavelengths of the second control wave (λ_{in} = 1554.4 nm, λ_{C1} = 1532.5 nm). (a) λ_{C2}=1550.5 nm, λ_{out}=1536.0 nm; (b) λ_{C2}=1548.6 nm, λ_{out}=1537.6 nm; (c) λ_{C2}=1545.3 nm, λ_{out}=1540.9 nm; (d) λ_{C2}=1541.0 nm, λ_{out}=1545.2 nm

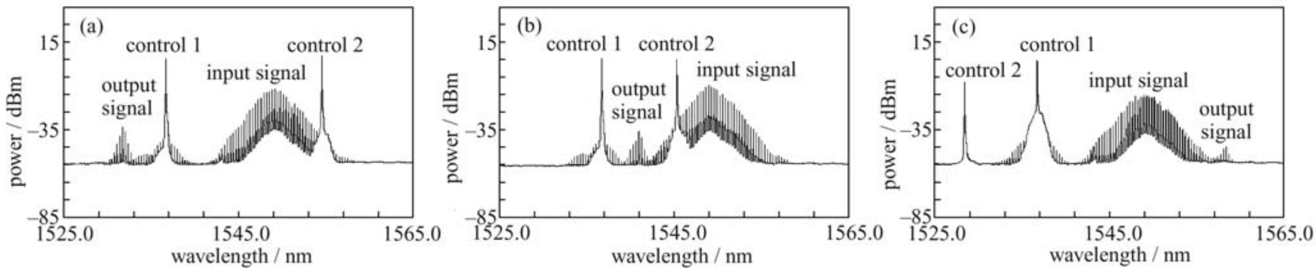

Fig. 4 Measured output spectra from tunable wavelength converter for different wavelengths of the second control wave when changing the signal wavelength (λ_{in} = 1548.9 nm, λ_{C1} = 1536.7 nm). (a) λ_{C2}=1554.5 nm, λ_{out}=1531.7 nm; (b) λ_{C2}=1545.2 nm, λ_{out}=1540.9 nm; (c) λ_{C2}=1528.4 nm, λ_{out}=1558.4 nm

level. Thus, it is easy to clearly observe the wavelength up-conversion as shown in Fig. 4(c).

Figure 5 further presents the measured output spectra for wavelength up-conversion. The second control wave is set within the short-waveband, and the output signal is obtained within the long-waveband. As shown in Figs. 5(a) and 5(b), for a fixed input signal, the first control wave is also unchanged. The wavelength of the output signal can be changed by adjusting the wavelength of the second control wave. For a variable input signal, as seen from Figs. 5(b)–5(d), it is still possible to obtain the tunable output of the converted output signal by appropriately adjusting the wavelengths of the first and the second control waves.

In the experiment, the measured output optical powers of the first and second control waves are about 2.4 and 4.8 dBm in Fig. 3, 5.7 and 6.5 dBm in Figs. 4(a) and 4(b), and 9.1 and 0.4 dBm in Fig. 5. The measured conversion efficiency is larger than −35 dB in Fig. 3 and larger than −30 dB in Figs. 4 and 5. The maximum conversion efficiency is measured to be larger than −22 dB, as shown in Fig. 4(a). Note that the difference of conversion efficiency in Figs. 3–5 can be ascribed to the power difference of two control waves and the power jitter of optical sources. On the other hand, variation of the polarization state during different time periods and the surrounding environment such as temperature are also regarded as important factors influencing the

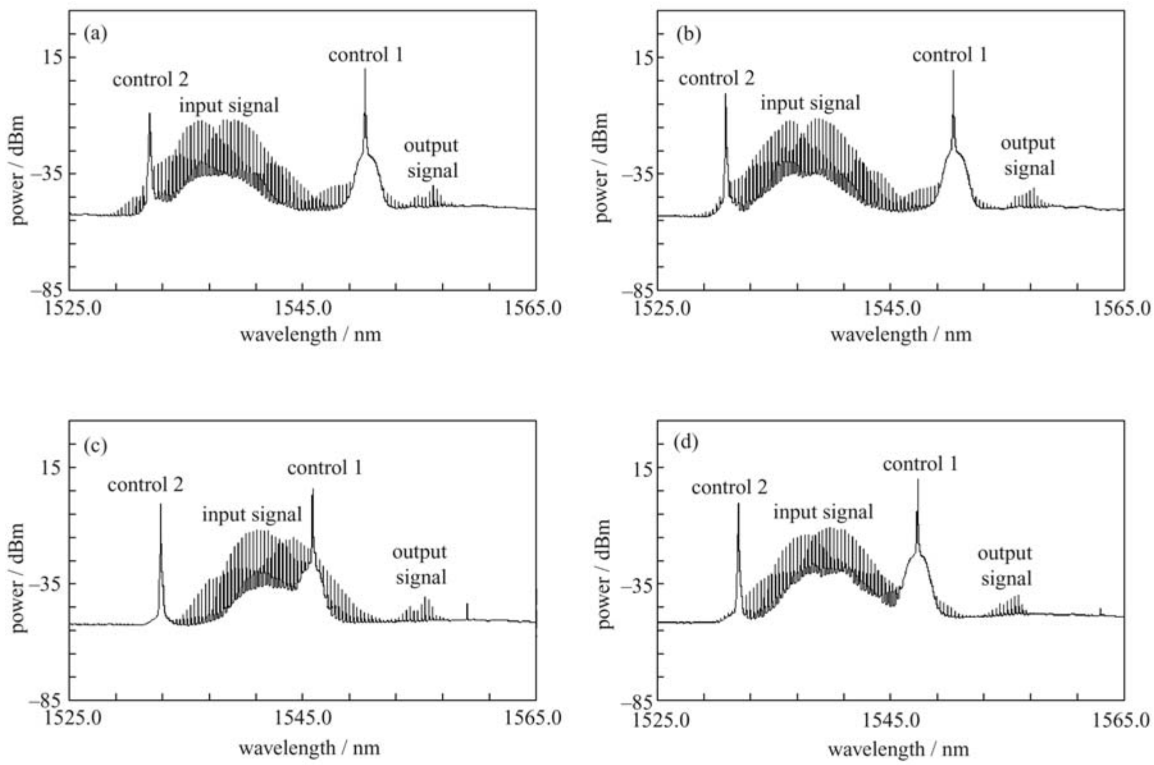

Fig. 5 Measured output spectra for wavelength up-conversion from tunable wavelength converter. (a) λ_{in}=1537.5 nm, λ_{C1}=1550.4 nm, λ_{C2}=1531.9 nm, λ_{out}=1556.2 nm; (b) λ_{in}=1537.5 nm, λ_{C1}=1550.4 nm, λ_{C2}=1530.8 nm, λ_{out}=1557.2 nm; (c) λ_{in}=1541.1 nm, λ_{C1}=1545.9 nm, λ_{C2}=1532.8 nm, λ_{out}=1555.5 nm; (d) λ_{in}=1539.8 nm, λ_{C1}=1547.3 nm, λ_{C2}=1532.0 nm, λ_{out}=1555.6 nm

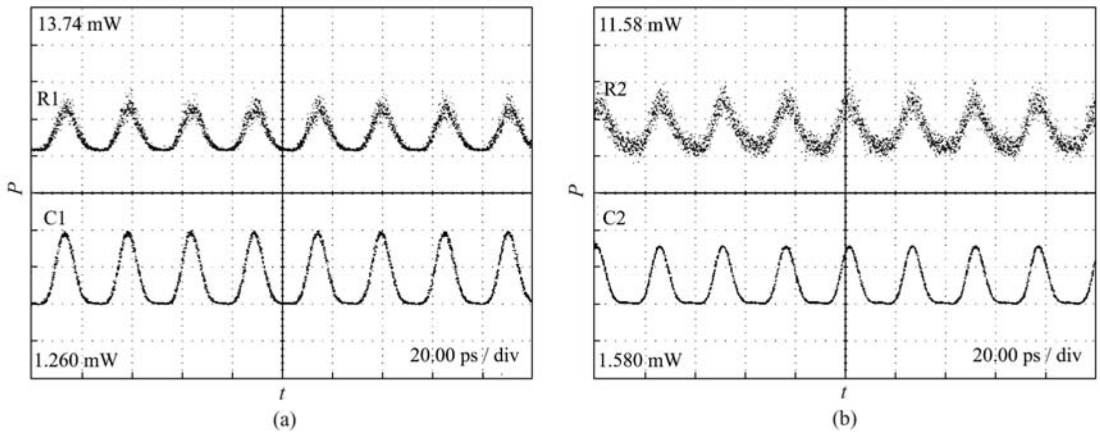

Fig. 6 Waveforms for output signal pulses (R1, R2) and input signal pulses (C1, C2). (a) Wavelength down-conversion shown in Fig. 4(a); (b) wavelength up-conversion shown in Fig. 5(d)

efficiency. Although the conversion efficiency in Figs. 3–5 is not very high, the converted output signal can still be clearly observed due to the very low ASE noise level.

Figures 6(a) and 6(b) plot the waveforms for the output signal and input signal corresponding to wavelength down-conversion and up-conversion, respectively. It is worth noting that the observed full-width at half maximum (FWHM) of the input signal shown in Fig. 6 is larger than the true value of 1.57 ps measured by the autocorrelator. Such phenomenon can be explained by the fact that the CSA used in the experiment is limited by the response speed of the installed photodetector. However, it does not affect the experimental observation on the successful realization of the wavelength conversion from the input signal to the output signal. By comparing the waveforms of the input and output signal as shown in Figs. 6(a) and 6(b), it can be clearly seen that the information carried by the input signal is completely copied onto the output signal. The abscissa scale in Fig. 6 is 20.00 ps/div, and there are 8 pulse trains within a time period of 200 ps, which indicates that the repetition rate of the input and output signals is 40 GHz. In addition, as can be seen from Figs. 6(a) and 6(b), the signal quality of the output signal for wavelength down-conversion is much better than that for wavelength up-conversion, which can be explained by the optical spectra shown in Fig. 4(a) and Fig. 5(d). The optical signal-to-noise ratio (OSNR) in dB of the output signal is defined as the subtraction of the noise power (dBm) from the output signal peak power (dBm), which can be calculated from the optical spectrum. For wavelength down-conversion as shown in Fig. 4(a), the second control wave is set within the gain range of EDFA, and therefore can be effectively amplified. Thus, large optical power of the output signal can be obtained, resulting in a high value of OSNR ($>$20 dB). On the contrary, for wavelength up-conversion as shown in Fig. 5(d), the second control wave is kept within the short-waveband and even far away from the gain range of EDFA. Therefore, without effective amplification of the second control wave, the optical power of the output signal is greatly reduced, and the OSNR of the output signal is low ($<$ 8 dB). As a result, a better performance of the wavelength down-conversion is obtained in comparison to the wavelength up-conversion because of the OSNR difference of the output signal. Nevertheless, simultaneous wavelength down- and up-conversions are still successfully observed due to the effective suppression of ASE noise.

5 Conclusions

In the present paper, a wavelength converter based on cSFG/DFG in a PPLN waveguide is experimentally investigated. Tunable wavelength conversion of picosecond pulsed signal with a pulse width of 1.57 ps and a repetition rate of 40 GHz is demonstrated in the experiment. By employing two narrow band tunable filters to effectively suppress ASE noise, simultaneous wavelength down- and up-conversions are experimentally observed.

Acknowledgements This work was supported by the National Natural Science Foundation of China (Grant No. 60577006).

References

1. Yoo S J B. Wavelength conversion technologies for WDM network applications. Journal of Lightwave Technology, 1996, 14(6): 955–966
2. Ellis A D, Kelly A E, Nesset D, et al. Error free 100 Gbit/s wavelength conversion using grating assisted cross-gain modulation in 2 mm long semiconductor amplifier. Electronics Letters, 1998, 34(20): 1958–1959
3. Joergensen C, Danielsen S L, Durhuus T, et al. Wavelength conversion by optimized monolithic integrated Mach-Zehnder

interferometer. IEEE Photonics Technology Letters, 1996, 8(4): 521–523
4. Højfeldt S, Bischoff S, Mørk J. All-optical wavelength conversion and signal regeneration using an electroabsorption modulator. Journal of Lightwave Technology, 2000, 18(8): 1121–1127
5. Liu W, Sun J Q. A novel scheme for polarization-insensitive optical wavelength conversion based on four-wave mixing in semiconductor optical amplifier. Acta Optica Sinica, 2001, 21(9): 1047–1051 (in Chinese)
6. Zhu X Z, Zhou J, Lou Q H, et al. Experimental investigation of quasi-CW frequency-doubling of broad band fiber laser in periodically poled lithium niobate. Acta Optica Sinica, 2004, 24(10): 1330–1334 (in Chinese)
7. Zhu X Z, Zhou J, Lou Q H, et al. 59 mW green light second harmonic generation of quasi-CW double-cladding fiber laser in periodically poled lithium niobate. Chinese Journal of Lasers, 2004, 31(7): 777–779
8. Zhang B G, Yao J Q, Zhang H, et al. Angle-tuned signal-resonated optical parametric oscillator based on periodically poled lithium niobate. Chinese Optics Letters, 2003, 1(6): 346–349
9. Chou M H, Hauden J, Arbore M A, et al. 1.5-μm-band wavelength conversion based on difference-frequency generation in $LiNbO_3$ waveguides with integrated coupling structures. Optics Letters, 1998, 23(13): 1004–1006
10. Zhou B, Xu C Q, Chen B. Comparison of difference-frequency generation and cascaded $\chi^{(2)}$ based wavelength conversions in $LiNbO_3$ quasi-phase-matched waveguides. Journal of the Optical Society of America B–Optical Physics, 2003, 20(5): 846–852
11. Chou M H, Brener I, Fejer M M, et al. 1.5-μm-band wavelength conversion based on cascaded second-order nonlinearity in $LiNbO_3$ waveguides. IEEE Photonics Technology Letters, 1999, 11(6): 653–655
12. Sun J Q, Liu W, Tian J, et al. Multichannel wavelength conversion exploiting cascaded second-order nonlinearity in $LiNbO_3$ waveguides. IEEE Photonics Technology Letters, 2003, 15(12): 1743–1745
13. Wang J, Sun J Q, Li J, et al. Single-to-dual channel wavelength conversion of picosecond pulses using PPLN-based double-ring fibre laser. Electronics Letters, 2006, 42(4): 236–238
14. Chen B, Xu C Q. Analysis of novel cascaded $\chi^{(2)}$ (SFG + DFG) wavelength conversions in quasi-phase-matched waveguides. IEEE Journal of Quantum Electronics, 2004, 40(3): 256–261
15. Yu S, Gu W. A tunable wavelength conversion and wavelength add/drop scheme based on cascaded second-order nonlinearity with double-pass configuration. IEEE Journal of Quantum Electronics, 2005, 41(7): 1007–1012
16. Lee Y L, Yu B-A, Jung C, et al. All-optical wavelength conversion and tuning by the cascaded sum- and difference frequency generation (cSFG/DFG) in a temperature gradient controlled Ti:PPLN channel waveguide. Optics Express, 2005, 13(8): 2988–2993
17. Wang J, Sun J Q, Luo C H, et al. Experimental demonstration of wavelength conversion between ps-pulses based on cascaded sum- and difference frequency generation (SFG + DFG) in $LiNbO_3$ waveguides. Optics Express, 2005, 13(19): 7405–7414
18. Min Y H, Lee J H, Lee Y L, et al. Tunable all-optical wavelength conversion of 5 ps pulses by cascaded sum- and difference frequency generation (cSFG/DFG) in a Ti:PPLN waveguide. In: Proceedings of Optical Fiber Communications Conference (OFC'03), Atlanta. 2003, 2: 767–768